Chitosan-Loaded Copper and Silver Nanocomposites as Antifungal Agents for Treatment of Pathogenic Fungi in Aquatic Environment

Ahmed M. Azzam[*]**, Bayaumy B. Mostafa, Mona B. Abd El-latif**

Environmental Research Department, Theodor Bilharz Research Institute (TBRI),
Giza, P.O. Box 30 No. 12411, Egypt.
*Corresponding authors: ah.azzam@tbri.gov.eg

ARTICLE INFO

ABSTRACT

The present work was designed for the formation of more active antifungal agents via loading copper (Cu) and silver (Ag) nanoparticles (NPs) on chitosan (CS) natural polymer. Sixty water and sediment samples were collected from Qalubiya, Egypt. One hundred and five fungal isolates were selected according to cultural characteristics, 53 isolates from sediment and 52 from water. Most isolates were identified as *Aspergillus* sp., *Penicillium* sp., *Candida* sp. and *Fusarium* sp. Nanocomposites (NC) of Cu@CS, Ag@CS, and Cu@Ag@CS were characterized by TEM, SEM, XRD and FTIR analysis for detecting their morphology and size, active surface groups and confirming its conjugation. The average sizes of these nanocomposites were 25, 19 and 33nm, with predominantly spherical shapes in aggregates, respectively. The antifungal study showed that the Cu@Ag@CS nanocomposite (NC) is a more effective and stable antifungal agent. For minimal fungicidal concentration (MFC) Cu@Ag@CS represented the lowest concentrations of 0.125, 0.25, 0.25 and 0.5 mg.ml^{-1} for *Candida* sp., *Aspergillus* sp., *Fusarium* sp. and *Penicillium* sp., respectively. In addition, the viable fungal counts (VFCs) of *Candida* sp. in water treated with Cu@Ag@CS NC was reached to complete inhibition in water after 18 hours, while the cell membrane and cellular contents of treated *Candida* sp. were destroyed causing cell death. Thus, loading of Cu and Ag nanoparticles on chitosan proved to form a more active antifungal agent suitable for treating pathogenic fungi in the aquatic environment.

Graphical Abstract
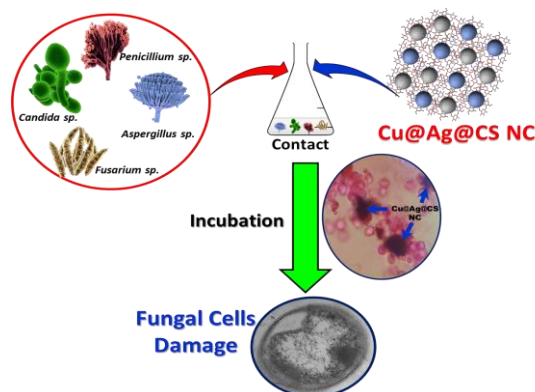
INTRODUCTION

Water is a radical element for living on earth, and the presence of microbes in water is a threat to this involvement. The transmission of pathogenic fungi from contaminated water to humans can cause health high-risk, especially for immunocompromised. Thus, the presence of pathogenic fungi in the aquatic

_____

environment has attracted great attention, and currently fungi are regarded as water contaminants affecting human health (**Hageskal** *et al.,* **2009; Shekha** *et al.,* **2013; Thomas & Thangavel, 2017; Góralska** *et al.,* **2020**).

It is worthy to mention that, sediment is the most adequate natural environment for the microbes' growth of bacteria, viruses, fungi and protozoa (**Anand** *et al.,* **2021; Kim** *et al.,* **2021; Liu** *et al.,* **2021; Stone** *et al.,* **2021**). Most fungal diseases are caused by sediment-borne fungi, which cause many diseases, whether for plants, animals or even humans for the sediment contains many fungal spores in a hidden way. Additionally, the presence of these germs in the agricultural sediment causes many losses in crops and lack of production and the consequent economic losses for farmers (**Shuping & Eloff 2017; Refai** *et al.,* **2022**). On the other hand, fungal infections in humans mostly arise from an external source in the surrounding environment inside the human body through ingestion, inhalation or wound contamination (**Rokas, 2022**). In the latest years, the fungal infection has remarkably increased (resulting in more than 1.6 million deaths annually) adding to the species of genus *Aspergillus*, *Candida*, *Penicillium*, *Cryptococcus*, *Fusarium*, *Mucor*, *Rhizopus*, etc… which appeared as the reason of many human infections (**Bandh** *et al.,* **2016; Barber** *et al.,* **2020;   Rokas, 2022**). Fungi have a great ability to break down herbicides, and they are the most resistant to many environmental stress factors (**Carranza** *et al.,* **2017**). There are many environmental fungi (in soil, water and air) that can infect humans such as *Aspergillus* sp. The heavy use of fungicides in the agricultural environment may lead to an increase in the resistance of environmental fungi and an increase in the ability of opportunistic fungi to infect humans with many serious diseases (**Barber** *et al.,* **2020**).

Fungi in water and sediment are found in the form of biofilms, reservoirs of microbes inside water and sediment; these membranes are surrounded by polymeric materials due to an extracellular matrix that acts as a protective shelter and makes them stable enough to resist physical forces (**Fulaz** *et al.,* **2019; Sharma** *et al.,* **2019; Afonso** *et al.,* **2020; El-Elimat** *et al.,* **2021**). In addition, these strong biofilms show high resistance to many antibiotics and can cause many infections (**Fan** *et al.,* **2021**). Because of the antibiotic resistance of microorganisms toward medical drugs, nanotechnology gives us a chance to solve this problem (**Kobayash & Nakazato, 2020; Li** *et al.,* **2020**). Metallic nanoparticles have been considered as new antimicrobial agents (Nano antibiotics). They have the tendency to resolve the mentioned resistance problem (**Lee** *et al.,* **2018; Qi** *et al.,* **2020**).

Copper and silver nanoparticles have well-known antimicrobial and cytotoxic behavior. Silver nanoparticles (Ag NPs) show a greater ability than silver ions against microbes because they have a large surface area and a surface with intense and active charges, and thus they are effective at very low concentrations (**Wu** *et al.,* **2018; Essghaier** *et al.,* **2022**). Copper has been used for more than four thousand years as a disinfectant and antimicrobial (**Hostynek & Maibach, 2004**). From there, copper nanoparticles (Cu NPs) have a great anti-fungal and anti-bacterial ability, as well as a low manufacturing cost (**Pham** *et al.,* **2019**). Therefore, in the field of combating fungal diseases in plants, copper nanoparticles are distinguished by their great efficiency in this field (**Pariona** *et al.,* **2019; Ibarra-Laclette** *et al.,* **2022**).

Modern strategies depend on reducing the toxic effects on human health or the environment through the production of antimicrobials based on nanomaterials because of their effectiveness at very low concentrations, making them less poisonous and eco-friendly (**Graves** *et al.,* **2017**). Therefore, many materials were used as stabilizing agents to maintain the effectiveness of nanometric particles for more time

with high activity, such as polysaccharides and polymers and combined with nanomaterials (**Bogdanova & Chvalun, 2016; Fan *et al.,* 2021; Sidhu *et al.,* 2022**).

Chitosan (CS) is a natural biopolymer found in the form of chitin in the shells of crustaceans and insects and is produced through the deacetylation process; it is an eco-friendly polymer (**Sun *et al.,* 2017**). CS-matrix has demonstrated antimicrobial properties against several microorganisms (**Li *et al.,* 2010; Hussein *et al.,* 2013; Sun *et al.,* 2022**). The unique structure of chitosan among natural polymers in particular has a great chelating ability (**Higazy *et al.,* 2010; Zhang *et al.,* 2018**). The synergistic design of biopolymer and metallic systems to produce nanocomposites is a major challenge, especially for broader applications. It has been reported that CS/metal ions after complexing showed great ability against microbial growth. This could be the result of the union of the common properties between the CS-matrix and the nanoparticles (**Brunel *et al.,* 2013; Gritsch *et al.,* 2018**).

This work aimed to fabricate chitosan-based nanocomposites copper@chitosan (Cu@CS), silver@chitosan (Ag@CS), and copper@silver@chitosan (Cu@Ag@CS) as more active eco-friendly antifungal agents and study their activities against some of the most prevalent pathogenic fungi isolated from aquatic Egyptian environment.

MATERIALS AND METHODS

Sampling, isolation and identification of fungi

Different locations in Qalubiya governorate, Egypt were chosen for sample collection. Sixty water and sediment samples were placed in sterile polyethylene cubs and bags and then transported to the laboratory (Environmental Research Department, Theodor Bilharz Research Institute, Egypt) and stored at a low temperature (4 °C) until examination.

After water samples were collected and transported to the lab, 100ml of each collected sample was filtrated using a membrane filter (0.45µm), and 10ml of sterile distilled water (DW) was used for diluting one gram of each collected sediment sample. One ml of filtrated water samples and sediment suspension were added to sterile Petri plates in triplicates containing sterile Sabouraud's Dextrose Agar (SDA), then plates were incubated at 28°C for 5-10 days (**Hageskal *et al.,* 2009**). Pure isolates culture were done using a test tube containing fresh agar slants of SDA. The test tubes were stored in the refrigerator. When inoculums were transferred into Petri plates containing nutrient media, cells were not separated from each other. Therefore, a spread plate technique was employed for pure culture (**Nacoon *et al.,* 2020**). Three triplicates were conducted per water and sediment source. All different purified fungal isolates on SDA were stored at -20°C for further identification.

The fungal isolates were identified morphologically according to **Barnett and Hunter (1998)**. The colonies that grew on the dishes were counted and then replanted until reaching the species level. Then, based on the macroscopic characteristics (pigmentation, topography, colony shape, and production of secretions) and microscopic characteristics (hyphal shape and spores), fungal isolates were identified according to **Howard (2002)** and **Watanabe (2002)**.

Chitosan (CS) extraction

Chitosan was extracted from the Egyptian shrimp shells and prepared according to **Manchanda (2022)**. Briefly, fresh shrimp shells were ground after being washed with distilled water and dried. The resulting powder was soaked in 1.0 M NaOH for 24 hours. The process of converting chitin to chitosan was carried out by

deacetylation through incubated powder for two hours in 50% NaOH at 115°C, and this process was repeated to complete chitosan purification. The resulting chitosan was rinsed well with distilled water and dried under a vacuum at 50°C and ground to fine particles and kept in a dry place.

Synthesis of copper nanoparticles (Cu NPs)

Cu NPs were prepared through the reduction of $CuSO_4$ solution by adding sodium borohydride solution slowly on a magnetic stirrer (5,000 rpm) for 60min. The dark blue precipitate was formed, and then filtered, washed and dried at 50°C overnight (**Suramwar et al., 2016**).

Synthesis of silver nanoparticles (Ag NPs)

Ag NPs were prepared through the reduction of silver nitrate solution by adding sodium borohydride solution slowly on a magnetic stirrer (5,000 rpm) for 60min. The dark brown precipitate was formed, and then filtered, washed and dried at 50°C overnight (**Mavani & Shah, 2013**).

Synthesis of copper@chitosan (Cu@CS) and silver@chitosan (Ag@CS) nanocomposites

Chitosan-based nanocomposites were prepared as the procedure described by **Abu-Elala et al. (2018)**. An acidic solution (2% acetic acid) was used to prepare the chitosan solution. Each of the copper and silver nanoparticles of ethanolic suspension were put in an ultrasonic device (Model 55743-Fritsch, Germany) for 20min. Then, each were added individually drop-by-drop to chitosan solution on a magnetic stirrer (5,000 rpm), and then left for about 4 hour- stirring. Both nanocomposites were precipitated by adding an alkaline solution to the mixture, and then filtered, washed until attaining a neutral pH and dried at 60°C.

Synthesis of copper@silver@chitosan (Cu@Ag@CS) nanocomposite

An amount of 1.0g of chitosan was dissolved in 2% of acetic acid water with an ultrasonic device. The solution was exposed to ultrasonic waves for 15min and then magnetically stirred at 5,000 rpm. In the meantime, sonicated solutions of silver and copper nanoparticles were added to the chitosan solution by stirring for 30min. After that, the glutaraldehyde solution was introduced to the mixture dropwise, and then the mixture was left stirring for about 6 hours at 5,000 rpm, as shown in Scheme (1) (**Liang et al., 2019**).

Characterization of synthesized nanocomposites

The evaluation of the morphology and particle size of fabricated nanocomposites, SEM (JEOL JSM-5600 LV) and transmission electron microscope (TEM, Philips EM208S, 100 kV Netherland) were used, and the average particle size was determined by ImageJ software. A drop of each nanocomposite suspension was placed in nickel grids for microscopic observation. X-ray diffraction analysis (XRD) was used for confirming successful conjugation between chitosan and Cu and Ag nanoparticles. To detect the interaction of surface functional groups and the formation of nanocomposites, the FTIR spectra of chitosan, Cu@CS, Ag@CS, and Cu@Ag@CS nanocomposites were analyzed.
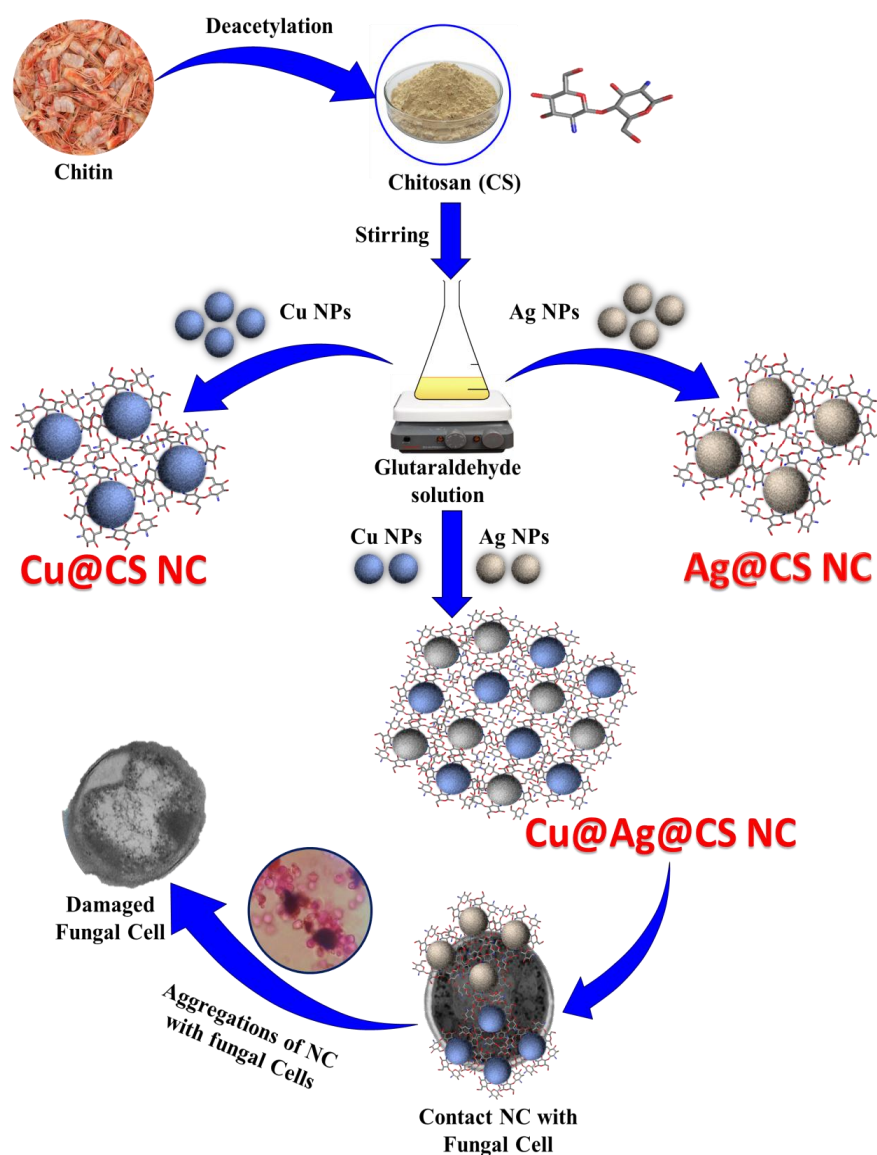
Scheme 1. Extraction of chitosan and fabrication of three chitosan-basid nanocomposites Cu@CS, Ag@CS, Cu@Ag@CS NCs and antifunagal activity of Cu@Ag@CS NC

Antifungal assay

Agar well diffusion method

The synthesized Cu@CS, Ag@CS, and Cu@Ag@CS nanocomposites were checked for antifungal activity using the agar well diffusion method. All the fungal strains were maintained in Sabouraud's dextrose agar. A 200μL of fungi inoculum was swabbed over the SDA plates using sterile buds. Different concentrations (0.5, 1.0, 2.0, 3.0, and 4.0 mg.ml^{-1}) of each synthesized nanocomposite were added to the wells formed on the SDA plates. Then, the plates were incubated at 28°C for 48 hours and then, the zones of inhibition were measured. Each experiment was performed in triplicate and the mean values ±SD were recorded following the instructions in the study of **Sabira *et al.* (2020)**.

_____

Minimal fungicidal concentration (MFC)

The MFC of Cu@CS, Ag@CS, and Cu@Ag@CS NCs was assayed for isolated fungi culture onto Sabouraud Dextrose agar plates for 2 days at 28°C for detecting the minimum concentration inhibiting the fungal growth on growth media (**Ashraf et al., 2020**). Different concentrations of each nanocomposite (from 0.125 to 2.0 mg/ml) were prepared and the lowest concentration of nanocomposites that have no growth of fungi was recorded as the minimum fungicidal concentration (MFC).

Viable fungal counts (VFCs) assay

Viable fungal counts (VFCs) assay was evaluated for unicellular fungus *Candida* sp. at different times after being treated with 1.0mg/ ml of Cu@Ag@CS NC, then the count of surviving *Candida* sp. was determined by plate count technique (triplicate) (**Azzam et al., 2022**). The mean values±SD of the reduction percentage of VFCs were calculated after treatment according to this formula:

$$\text{VFCs Reduction \%} = \frac{\text{Viable count at time0} - \text{Viable count at time x}}{\text{Viable count at time 0}} \times 100 \qquad (1)$$

Where, Time^0 is the time before adding Cu@Ag@CS NC, and Time^x is the contact time between fungus and nanocomposite.

Morphological futures of treated fungi

The effect of Cu@Ag@CS nanocomposite on the treated unicellular fungus *Candida* sp. was studied to mediate morphological changes and cell damage using both TEM and light microscopes. After exposing fungal cells to nanocomposite, cells were fixed in 1% glutaraldehyde then washed in 0.1M buffer, and 1% osmium tetraoxide was used for post-fixations and again washed with 0.1M buffer. The samples were dehydrated in acetone, infiltrated and embedded in epoxy resin. Slices of 60nm thickness were made using a diamond knife. The slices were put on copper grids and stained with uranyl acetate. Finally, the grids were dried in a desiccator and examined using TEM at 80 kV to study morphological changes due to the biocidal action of Cu@Ag@CS NC (**Azzam et al., 2019**). For light microscopes samples, the cells were examined under high powered field (HPF) (×100) after staining with safranin.

RESULTS AND DISCUSSION

Isolated fungi

In the present study, morphological techniques were used to identify the fungal isolates. Fig. (1) shows the numbers and percentages of fungal isolates from sediment and water samples. Four fungal species were found in thirty sediment samples, such as *Aspergillus* sp. (n=21 & 70%), *Penicillium* sp. (n=14 & 46.7%), *Candida* sp. (n=10 & 33.3%) and *Fusarium* sp. (n=8, 26.7%), while for other thirty water samples, three fungal species were identified including *Aspergillus* sp. (n=27 & 90%), *Penicillium* sp. (n=18 & 60%) and *Candida* sp. (n=7 & 23.3%). Moreover, Fig. (1A) presents the total number of four fungal species in sixty collected sediment and water samples, where *Aspergillus* sp., *Penicillium* sp., *Candida* sp. and *Fusarium* sp. recorded 48, 39, 17 and 8 isolates, respectively. However, Fig. (1B) shows the percent of each fungal species from 112 total isolates, where *Aspergillus* sp., *Penicillium* sp., *Candida* sp. and *Fusarium* sp. presented 42.9%, 34.8%, 15.2%, and 7.1% isolates, respectively. Thus, the species *Aspergillus* sp. and *Penicillium* sp. were most prevalent in water than sediment; conversely, *Candida* sp. and *Fusarium* sp. were most prevalent in

sediment than water (**Seth *et al.,* 2016; Raja *et al.,* 2017; Al-Bedak *et al.,* 2020; Góralska *et al.,* 2020; Monapathi *et al.,* 2021**).
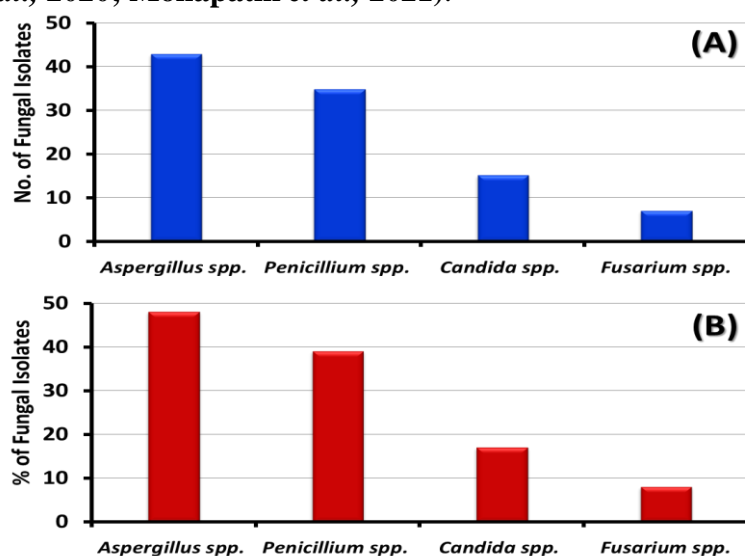
Fig. 1. A) Number of fungal isolates in total collected samples, and **B**) Percent of fungal isolate for all total isolates.

Characterization of nanocomposites

In this work, the conventional reduction method was used for the preparation of Cu NPs and Ag NPs, and then was conjugated with extracted chitosan (CS) to prepare Cu@CS, Ag@CS, and Cu@Ag@CS NCs, as shown in Scheme (1). Figs. (2, 3) display the SEM and TEM images of three nanocomposites, where the average sizes of Cu@CS, Ag@CS, and Cu@Ag@CS NCs were 25, 19 and 33nm, respectively. According to microphotographs, the Cu and Ag nanoparticles have predominantly spherical form, polydispersity character and slightly uniform distribution in the chitosan matrix. However, Cu@Ag@CS NC was spherical nanoparticles that can be observed in the scale bar of TEM embedded in chitosan; this result is agrees with that of **Ashraf *et al.* (2020)**.
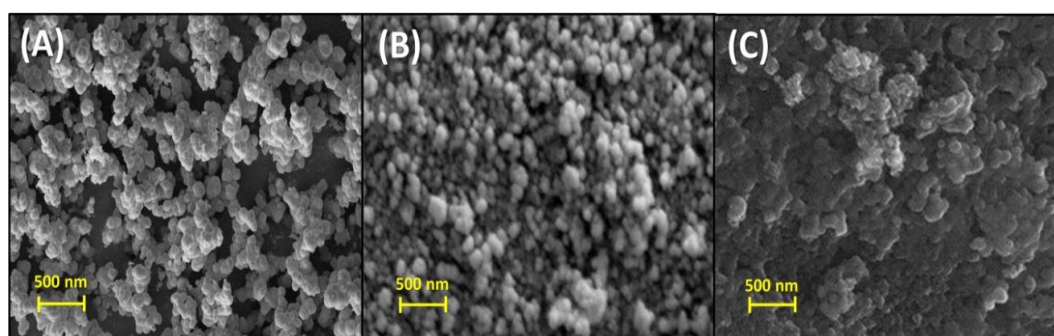
Fig. 2. SEM images of A) Cu@CS; B) Ag@CS; and C) Cu@Ag@CS nanocomposites.

_____
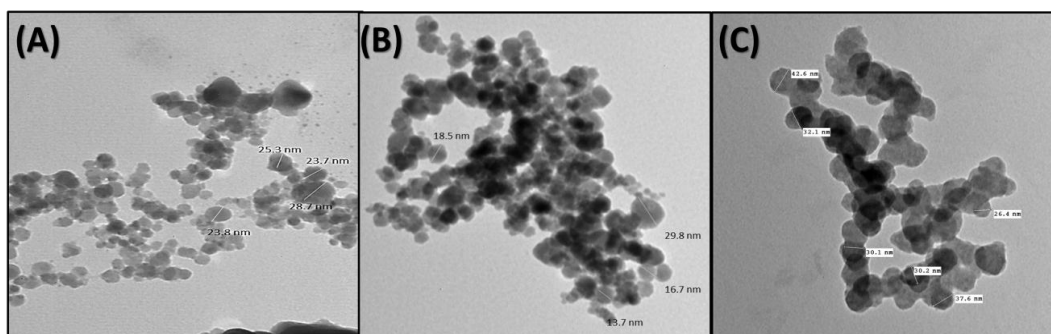
Fig. 3. TEM images of A) Cu@CS; B) Ag@CS; and C) Cu@Ag@CS nanocomposites.

The XRD pattern of chitosan indicated that the characteristic peaks were around $2\theta=10^o$ and 20° (Fig. 4). The XRD patterns of Cu@CS nanocomposites showed an amorphous part of chitosan. Moreover, these patterns revealed characteristic peaks located at 43.4^o and 50.4^o, which revealed the crystalline peaks (111, 200 and 220) of copper metal, respectively. The current characteristic results for Cu@CS NC nearly match with those of **Ashraf *et al.* (2020)** and **Ghafarzadeh *et al.* (2023)**.

The XRD pattern of Ag@CS is shown in Fig. (4), which clearly show the formation of silver metal. Peaks were located at values of 39.9^o, 43.5^o and 61.2^o, corresponding to 111, 200 and 220, respectively, which coincide with that of the JCPDS card No. 89-3722 **(Badawy *et al.*, 2019)**; additionally, a peak for chitosan appeared at a value of 19.7^o, which agrees with previous results of **Ghafarzadeh *et al.* (2023)**. The characteristic peaks for copper and silver and the two characteristic peaks of chitosan at $2\theta=18.7^o$ and 11.3^o are shown in Fig. (4), which indicate the successful fabrication of Cu@Ag@CS nanocomposite.

Fig. 4. XRD of chitosan, Cu@CS, Ag@CS, and Cu@Ag@CS nanocomposites

The interaction of functional groups and the formation of the end product were analyzed by FTIR, as shown in Fig. (5). For chitosan, a wide band at 3425 cm^{-1} was specified for superposition between the O−H protracting vibration and the N−H

stretching vibration. However, the hand at $2928cm^{-1}$ represented the aliphatic C−H bonds. The peaks appearing at $1653cm^{-1}$ and $1612cm^{-1}$ corresponded to the stretching of the amide I, II and III bonds. The peaks of −OH and −NH$_2$ appeared at $3425cm^{-1}$ due to combining groups stretching in chitosan. Moreover, peaks at 1653, 1415 and 710 cm^{-1} represented the –CONH$_2$, C-N (I amine) and anhydrous glucosidic bonds, respectively (Fig. 5a) (**Choudhary *et al.*, 2019**).

In Cu@CS NC (Fig. 5b), these peaks had more characteristic with slight move to 3427, 1634, 1409, and 631 cm^{-1}, which confirms strong bonding and the presence of chitosan (**Lonĉarević *et al.*, 2021**). As shown in Fig. (5c), the spectra of Ag@CS NC showed fewer chitosan characteristic peaks, whereas chitosan bands at 1653 cm^{-1} and 1612 cm^{-1} were shifted to 1638 cm^{-1} due to stretching vibrations of amide C=O bonds and transmittance decreasing of band region. The Ag NPs chelated with chitosan amino and hydroxyl groups were confirmed through the intensity of N−H and O−H that stretched and presented at $3425cm^{-1}$. The disappearance of the NH$_2$ double peak and the appearance of functional groups on the surface of the Ag NPs indicate the success of the bonding of the Ag NPs with chitosan (**Lunkov *et al.*, 2022**). FT-IR spectra of Cu@Ag@CS NC in Fig. (5d) show related bands to Cu–O and Ag–O at regions of 647 and 457 cm^{-1}, which confirmed the presence of copper and silver in the structure of nanocomposite. Furthermore, the peaks at $1007cm^{-1}$ (C–O–C) and $1350cm^{-1}$ (C–O) were related to the presence of chitosan in the nanocomposite (**Song *et al.*, 2022**).

Fig. 5. FTIR spectra of a) Chitosan, b) Cu@CS, c) Ag@CS, and d) Cu@Ag@CS nanocomposites

Antifungal assay

The antifungal activity of three synthesized nanocomposites was investigated against the four isolated fungi (*Aspergillus* sp., *Penicillium* sp., *Candida* sp. and *Fusarium* sp.), using a well diffusion assay. The antifungal activity was determined based on the inhibition zones (IZ) of different concentrations (1, 2, 3, 4 mg.ml^{-1}). Fig. (6A) shows the results, where the diameters of IZ at concentration 4.0 mg.ml^{-1} of

Cu@CS NC were 16, 15.5, 14.5 and 17mm against *Aspergillus* sp., *Penicillium* sp., *Candida* sp. and *Fusarium* sp., respectively, while with the same concentration of Ag@CS, NC represented 15, 13, 12.5 and 14mm, respectively (Fig. 6B). This indicates that Cu@CS NC was more active than Ag@CS NC against tested fungal species. Moreover, Cu@Ag@CS NC was more active than two single nanocomposites, where at concentration 4.0 mg.ml^{-1}, it recorded inhibition zones of 17, 18.5, 21 and 18mm with fungal species, respectively (Fig. 6C). These outcomes mean that the antifungal activities were dosage-dependent, where the inhibition zones diameters increased by increasing the concentration of the nanocomposites from 1.0 to 4.0 mg.ml^{-1}, as shown in Fig. (6), which concurs with the results of **Arya *et al.* (2019)**, **Wichai *et al.* (2019)** and **Sabira *et al.* (2020)**.
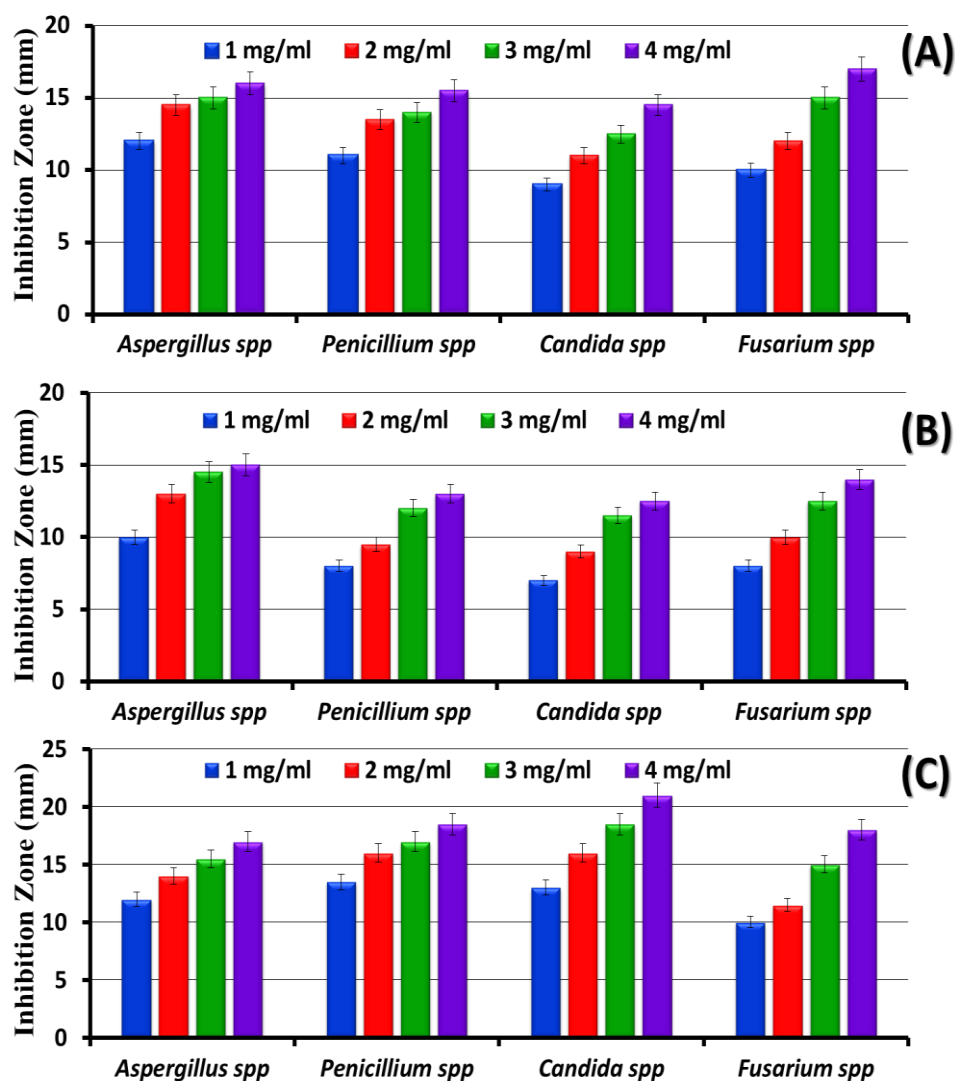
Fig. 6. Inhibition zones of **A)** Cu@CS; **B)** Ag@CS; and **C)** Cu@Ag@CS nanocomposites against tested fungal species

Minimal fungicidal concentration (MFC) of nanocomposites

Fig. (7A) exhibits the MFC concentrations of the synthesized three nanocomposites against *Candida* sp. fungal species, where MFC of Cu@CS NC against *Aspergillus* ssp., *Candida* sp., *Fusarium* sp. and *Penicillium* sp. were recorded as 0.5, 0.5, 0.5 and 0.75 mg.ml^{-1}, respectively, while MFC of Ag@CS NC were 0.75, 0.75, 0.5, and 1.0

mg.ml^{-1}, respectively. Moreover, MFC of Cu@Ag@CS NC represented concentrations 0.125, 0.25, 0.25 and 0.5 mg.ml^{-1} against *Candida* sp., *Aspergillus* ssp., *Fusarium* sp. and *Penicillium* sp., respectively (Table S5) **(Ashrafi *et al.,* 2020)**.

Viable fungal counts (VFCs) assay

Fig. (7B) shows the reduction percent of viable *Candida* sp. fungal counts (VFCs) treated with 1.0 mg.ml^{-1} of Cu@Ag@CS NC at different contact times, where after 1.0 hour of contact time, 25% of fungal cells were reduced. While, after 12 hours, they reached 96%. However, complete inhibition was recorded after 18 hours of treatment **(Ashrafi *et al.,* 2020)**.
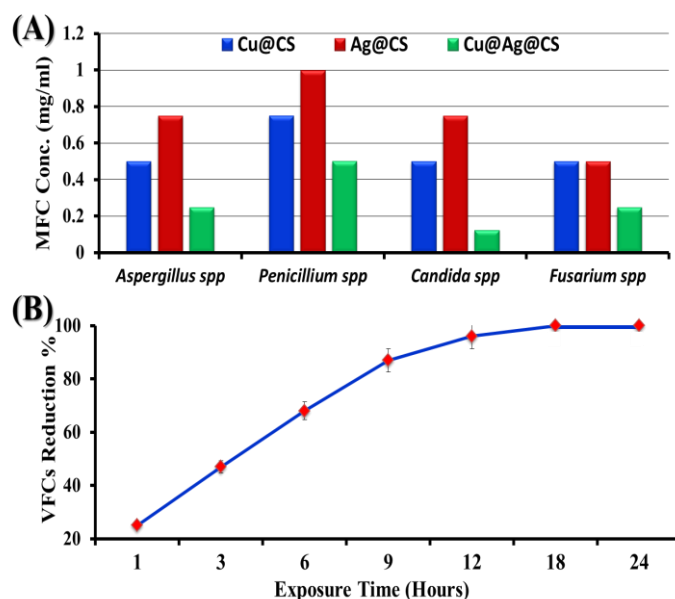
Fig. 7. A) Minimal fungicidal concentration (MFC) of Cu@CS, Ag@CS, and Cu@Ag@CS nanocomposites against tested fungal species; **B)** Reduction percent in viable fungal counts (VFCs) of *Candida* sp. treated with Cu@Ag@CS NC at different contact times

Morphological futures of treated unicellular fungi

As a result of using antifungal Cu@Ag@CS nanocomposite, the cell wall was broken leading to cell death. Moreover, SEM images revealed the reaction between this nanocomposite and *Candida* sp. cells and its membrane structure after being exposed to 1.0 mg.ml^{-1}. Fig. (8A, B) show great changes in the cell membranes, the formation of holes and pores in the cell wall, affecting their internal contents and subsequently causing death. These outcomes provide a detailed explanation of the damages caused to the cells as a result of the significant effect of the nanocomposite, which explains the way the *Candida* sp. cells were affected and the stress they were exposed to. Additionally, the light microscopic images in Fig. (8C, D) show fungal cell damage due to cell membrane disorders **(Ashrafi *et al.,* 2020; Elbahnasawy *et al.,* 2021)**.
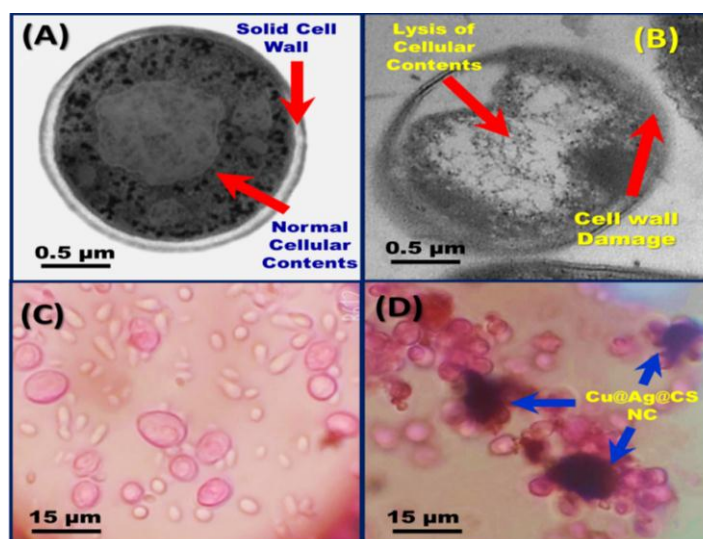
Fig. 8. Transmission electron micrographs and light microscopic images of *Candida* spp. Cells**.** (**A &** **C**) untreated; (**B & D**) treated with Cu@Ag@CS nanocomposites.

CONCLUSION

The present work describes a cost-effective facile synthesis of a more active antifungal agent for the treatment of pathogenic environmental fungi. The copper@silver@chitosan nanocomposite showed considerable antifungal activity against isolated fungi from sediment and water environment, whereas its activity was more than these of Cu@CS or Ag@CS NCs against tested fungi *Aspergillus* sp., *Candida* sp., *Fusarium* sp. and *Penicillium* sp. Moreover, Cu@Ag@CS NC completed inhibition for the unicellular fungus *Candida* sp. in less than 18 hours. However, the interaction between this nanocomposite and *Candida* sp. cells led to the lysis of its cell membrane and destroyed its intracellular contents causing cell death. Consequently, Cu@Ag@CS NC could be a successful alternative agent to combat pathogenic environmental fungi.

ACKNOWLEDGEMENTS

REFERENCES

Abu-Elala, M.N.; Abu Bakr, H.O.; Khattab, M.S.; Mohamed, S.H.; El-hadye, M.A.; Ghandour, R.A. and Mors, R.E. (2018). Aquatic environmental risk assessment of chitosan/silver, copper and carbon nanotube nanocomposites as antimicrobial agents. Inter. J. Bio. Macromol., 113:1105–1115.

Afonso, T.B.; Simoes, L.C. and Lima, N. (2020). Occurrence of filamentous fungi in drinking water: their role on fungal-bacterial biofilm formation. Res. Micro. 172(1): 103791-103800.

Al-Bedak, O.; Moubasher, A.; Ismail, M. and Mohamed, R. (2020). *Aspergillus curvatus*, a new species in section *Circumdati* isolated from an alkaline water of Lake Khadra in Wadi-El-Natron, Egypt. Asian Journal of Mycology, 5: 325-334.

Anand, U.; Bianco, F.; Suresh, S.; Tripathi, V.; Núñez-Delgado, A. and Race, M. (2021). SARS-CoV-2 and other viruses in soil: An environmental outlook. Environmental Research, 198: 111297-111310.

Arya, G., Sharma, N., Mankamna, R. and Nimesh, S. (2019). In: Prasad, R. (Eds) Microbial Nanobionics. Nanotechnology in the Life Sciences. Springer Cham, pp. 89–119.

Ashraf, H.; Anjum, T.; Riaz, S. and Naseem, S. (2020). Microwave-assisted green synthesis and characterization of silver nanoparticles using melia azedarach for the management of *Fusarium* wilt in Tomato. Front. Microbiol., 11: 238-259.

Ashrafi, M.; Bayat, M.; Mortazavi, P.; Hashemi, S.J. and Meimandipour, A. (2020). Antimicrobial effect of chitosan–silver–copper nanocomposite on *Candida albicans*. J. Nanostruct. Chem., 10: 87–95.

Azzam, A.M.; Shenashen, M.A.; Mostafa, B.B.; Kandeel, W.A. and El-Safty, S.A. (2019). Antibacterial activity of magnesium oxide nanohexagonal sheets for wastewater remediation. Environ. Prog. Sust. Energ., 38(S1): 260-266.

Azzam, A.M.; Shenashen, M.A.; Selim, M.S.; Mostafa, B.; Tawfik, A. and El-Safty, S.A. (2022). Vancomycin-loaded furriness amino magnetic nanospheres for rapid detection of gram-positive water bacterial contamination. Nanomat., 12: 510-524.

Badawy, M.E.I.; Lotfy, T.M.R. and Shawir, S.M.S. (2019). Preparation and antibacterial activity of chitosan-silver nanoparticles for application in preservation of minced meat. Bull. Natl. Res. Cent., 43: 83-96.

Bandh, S.A.; Kamili, A.N.; Ganai, B.A. and Lone, B.A. (2016). Opportunistic fungi in lake water and fungal infections in associated human population in Dal Lake, Kashmir. Microb. Pathog., 93: 105-110.

Barber, A.E.; Riedel, J.; Sae-Ong, T.; Kang, K.; Brabetz, W.; Panagiotou, G.; Deising, H.B. and Kurzaia O. (2020). Effects of agricultural fungicide use on *Aspergillus fumigatus* Abundance, Antifungal Susceptibility, and Population Structure. Amr. Soc. Microbiol., mBio., 11(6): 02213-02220.

Barnett, H.L. and Hunter, B.B. (1998). Illustrated Genera of Imperfect Fungi. 4th Edition, APS Press, St. Paul, 1-218.

Bogdanova, O.I. and Chvalun, S.N. (2016). Polysaccharide-based natural and synthetic nanocomposites. Polym. Sci. Ser. A, 58: 629–658,

Brunel, F.; Gueddari, N.E. and Moerschbacher, B.M. (2013). Complexation of copper (II) with chitosannanogels: Toward control of microbial growth. Carbohydr. Polym., 92 :1348–1356.

Carranza, C.S.; Barberis, C.L; Chiacchiera, S.M. and Magnoli, C.E. (2017). Assessment of growth of *Aspergillus* spp. from agricultural soils in the presence of glyphosate. Rev. Argent. Microbiol., 49(4): 384-393.

Choudhary, R.C.; Kumari, S.; Kumaraswamy, R.V.; Pal, A.; Raliya, R.; Biswas, P. and Saharan, V. (2019). Characterization methods for chitosan-based NMs. Plant nanobionics. Springer, Cham.: 103–116.

Elbahnasawy, M.A.; Shehabeldine, A.M.; Khattab, A.M.; Amin, B.H. and Hashem, A.H. (2021). Green biosynthesis of silver nanoparticles using novel endophytic *Rothia endophytica*: Characterization and anticandidal activity. J. Drug Deliv. Sci. Techn. 62: 102401-102416.

El-Elimat, T.; Raja, H.A.; Figueroa, M.; Al-Sharie, A.H.; Bunch, R.L. and Oberlies, N.H. (2021). Freshwater fungi as a source of chemical diversity: A Review. J. Nat. Prod., 84(3): 898–916.

Essghaier, B.; Khedher, G.B.; Hannachi, H.; Dridi, R.; Zid M.F. and Chaffei, C. (2022). Green synthesis of silver nanoparticles using mixed leaves aqueous extract of wild olive and pistachio: characterization, antioxidant, antimicrobial and effect on virulence factors of *Candida*. Archives of Microbiology, 204: 203-215.

Fan, X.; Yahia, L. and Sacher, E. (2021). Antimicrobial properties of the Ag, Cu nanoparticle system. Biology, 10: 137-173.

Fulaz, S.; Vitale, S.; Quinn, L. and Casey, E. (2019). Nanoparticle-biofilm interactions: The role of the EPS matrix. Trends Microbiol., 27: 915–926.

Ghafarzadeh, M.; Kharaziha, M.; Atapour, M. and Heidari, P. (2023). Copper-chitosan nanoparticles incorporated PGS/MAO bilayer coatings for potential cardiovascular application. Prog. Org. Coat., 174: 107269-10741.

Góralska, K.; Błaszkowska, J. and Dzikowiec, M. (2020). The occurrence of potentially pathogenic filamentous fungi in recreational surface water as a public health risk. Journal of Water and Health, 18(2): 127 – 144.

Graves, J.L.; Thomas, M. and Ewunkem, J.A. (2017). Antimicrobial nanomaterials: why evolution matters. Nanomater., 7: 283-292.

Gritsch, L.; Lovell, C.; Goldmann, W.H. and Boccaccini, A.R. (2018). Fabrication and characterization of copper(II)-chitosan complexes as antibiotic-free antibacterial biomaterial. Carbohydr. Polym., 179: 370–378.

Hageskal, G.; Lima, N. and Skaar, I. (2009). The study of fungi in drinking water. Mycol. Res., 113: 165-172.

Higazy, A.; Hashem, M.; ElShafei, A.; Shaker, N. and Hady, M.A. (2010). Development of antimicrobial jute packaging using chitosan and chitosan–metal complex. Carbohydr. Polym., 79: 867–874.

Hostynek, J.J. and Maibach, H.I. (2004). Skin irritation potential of copper compounds. Toxicol. Mech. Methods, 14: 205–213.

Howard, A.G. (2002). Water Supply Surveillance: A Reference Manual. WEDC, Loughborough University, 248pp

Hussein, M.H.M.; El-Hady, M.F.; Shehata, H.A.H.; Hegazy, M.A. and Hefni, H.H.H. (2013). Preparation of some eco-friendly corrosion inhibitors having antibacterial activity from sea food waste. J. Surfactants Deterg., 16: 233–242.

Ibarra-Laclette, E.; Blaz, J.; Pérez-Torres, C.; Villafán, E.; Lamelas, A.; Rosas-Saito, G.; Ibarra-Juárez, L.A.; García-Ávila, C.J.; Martínez-Enriquez, A.I. and Pariona, N. (2022). Antifungal effect of copper nanoparticles against *Fusarium kuroshium*, an obligate symbiont of *Euwallacea kuroshio* ambrosia beetle. J. Fungi, 8: 347-364.

Kim, L.; Yan, T.; Yost, R. and Porter, G. (2021). A sustainable and low-cost soil filter column for removing pathogens from Swine wastewater: The role of endogenous soil protozoa. Water, 13(18): 2472-2485.

Kobayashi, R.K.T. and Nakazato, G. (2020). Editorial: Nanotechnology for antimicrobials. Front. Microb., 11: 1421- 1423.

Lee, N.Y.; Hsueh, P.R. and Ko, W.C. (2018). Nanoparticles in the treatment of infections caused by multidrug-resistant organisms. Front. Pharmacol., 10: 1153-1162.

Li, L.; Deng, J.; Deng, H.; Liu, Z. and Xin, L. (2010). Synthesis and characterization of chitosan/ZnO nanoparticle composite membranes. Carbohydrate Research, 345: 994–998.

Li, Y.; Xiao, P.; Wang, Y. and Hao, Y. (2020). Mechanisms and control measures of mature biofilm resistance to antimicrobial agents in the clinical context. ACS Omega, 5: 22684–22690.

Liang, J.; Wang, J.; Li, S.; Xu, L.; Wang, R.; Chen, R. and Sun, Y. (2019). The size-controllable preparation of chitosan/silver nanoparticle composite microsphere and its antimicrobial performance. Carbohyd. Polym., 220: 22–29.

Liu, Y.; Eldridge, D.J.; Zeng, X.; Wang, J.; Singh, B.K. and Delgado-Baquerizo M. (2021). Global diversity and ecological drivers of lichenised soil fungi. New Phytologist, 231: 1210–1219.

Lonĉarević, A.; Ivanković, M. and Rogina, A. (2021). Electrosprayed chitosan–copper complex microspheres with uniform size. Materials, 14(19): 5630-5645.

Lunkov, A.; Shagdarova, B.; Lyalina, T.; Dubinnyi, M.A.; Karpova, N.; Lopatin, S.; Il'ina, A. and Varlamov, V. (2022). Simple method for ultrasound assisted «click» modification of azido-chitosan derivatives by CuAAC. Carbohyd. Polym., 282: 119109-119126.

Manchanda, S. (2022). Separation of chitin from shrimp and application in heavy metal wastewater treatment. J. Innov. Social Sci. Res., 9: 23-26.

Mavani, K. and Shah, M. (2013). Synthesis of silver nanoparticles by using sodium borohydride as a reducing agent. Int. J. Eng. Res. Technol., 2(3): 1–5.

Monapathi, M.; Oguegbulu, J.; Adogo, L.; Klink, M.J.; Okoli, B.; Mtunzi, F.; Modise, J. and Okoli, J. (2021). Pharmaceutical pollution: Azole antifungal drugs and resistance of opportunistic pathogenic yeasts in wastewater and environmental water. Appl. Environ. Soil Sci., 2021: 1-11.

Nacoon, S.; Jogloy, S.; Riddech, N.; Mongkolthanaruk, W.; Kuyper, T.W. and Boonlue, S. (2020). Interaction between phosphate solubilizing bacteria and arbuscular mycorrhizal fungi on growth promotion and tuber inulin content of *Helianthus tuberosus L.* Sci. Rep. 10(1): 4916-4925.

Pariona, N.; Mtz-Enriquez, A.I.; Sánchez-Rangel, D.; Carrión, G.; Paraguay-Delgado, F. and Rosas-Saito, G. (2019). Green-synthesized copper nanoparticles as a potential antifungal against plant pathogens. RSC Adv., 9: 18835–18843.

Pham, N.; Duong, M.; Le, M.; Hoang, H.A. and Pham, L.K.O. (2019). Preparation and characterization of antifungal colloidal copper nanoparticles and their antifungal activity against *Fusarium oxysporum* and Phytophthoracapsici. Compt. Rend. Chimi., 22: 786 – 793.

Qi, Y.; Ye, J.; Ren, S.; Lv, J.; Zhang, S.; Che, Y. and Nin, G. (2020). *In-situ* synthesis of metal nanoparticles@metal−organicframeworks: Highly effective catalytic performance and synergistic antimicrobial activity. J. Hazard. Mater., 387: 121687-121687-121703.

Raja, M.; Praveena, G. and William, S. J. (2017). Isolation and identification of fungi from soil in Loyola college campus, Chennai, India. Inter. J. Curr. Microbiol. App. Sci., 6(2): 1789- 1795.

Refai, T.; Ali, I.N.M.; Abdel-Nabi H.M.M.; Aly, A.A.; Khalil, M.I.I. and Abd-Elsalam, K.A. (2022). Pathogenicity assay of some soil-borne fungi isolated from cotton seedlings Egypt. J. Agric. Res., 100 (1): 41-48.

Rokas, A. (2022). Evolution of the human pathogenic lifestyle in fungi. Nat. Microb., 7: 607–619.

Sabira, S.F.; Kasabe, A.M.; Mane, P.C.; Chaudhari, R.D. and Adhyapak, P.V. (2020). Selective antifungal and antibacterial activities of Ag-Cu and Cu-Ag

core–shell nanostructures synthesized *in-situ* PVA. Nanotech., 31(48): 485705.

Seth, R.K.; Alam, S. and Shukla, D.N. (2016). Isolation and identification of soil fungi from wheat cultivated area of *Uttar pradesh*. J. Plant Pathol. Microbiol., 7(11): 1000384-1000386.

Sharma, D.; Misba, L. and Khan, A.U. (2019). Antibiotics versus biofilm: An emerging battleground in microbial communities. Antimicrob. Resist. Infect. Control., 8: 1–10.

Shekha, Y.A.; Ismael, H.M. and Ahmed, A.A. (2013). Bacteriological and mycological assessment for water quality of Duhok Reservoir, Iraq. Jordan J. Biol. Sci., 6(4): 308-315.

Shuping, D.S.S. and Eloff, J.N. (2017). The use of plants to protect plants and food against fungal pathogens: A review. Afr. J. Tradit. Compl. Altern. Med., 14(4): 120–127.

Sidhu, A.K.; Verma, N. and Kaushal, P. (2022). Role of biogenic capping agents in the synthesis of metallic nanoparticles and evaluation of their therapeutic potential. Front. Nanotech., 3: 801620-801636.

Song, J.; Cao, X. and Huang, Z. (2022). Diatomite-chitosan composite with abundant functional groups as efficient adsorbent for vanadium removal: Key influencing factors and influence of surface functional groups. J. Molec. Liq. 367(A): 120428-120443.

Stone, B.W.; Li, J.; Koch, B.J.; Blazewicz, S.J.; Dijkstra, P.; Hayer, M.; Hofmockel, K.S.; Liu, X.A.; Mau, R.L.; Morrissey, E.M.; Pett-Ridge, J.; Schwartz, E. and Hungate, B.A. (2021). Nutrients cause consolidation of soil carbon flux to small proportion of bacterial community. Nat. Communicat., 12: 3381-3389.

Sun, X.; Yin, L.; Zhu, H.; Zhu, J.; Hu, J.; Luo, X.; Huang, H. and Fu, Y. (2022). Enhanced antimicrobial cellulose/chitosan/ZnO biodegradable composite membrane. Membranes, 12: 239-251.

Sun, Y.; Zhu, C.; Sun, W.; Xu, Y.; Xiao, X. and Zheng, H. (2017). Plasma-initiated polymerization of chitosan-based CS-g-P (AM-DMDAAC) flocculant for the enhanced flocculation of low-algal-turbidity water. Carbohyd. Polym., 164: 222–232.

Suramwar, N.V.; Thakare, S.R. and Khaty, N.T. (2016). One pot synthesis of copper nanoparticles at room temperature and its catalytic activity. Arab. J. Chem., 9: S1807–S1812.

Thomas, M. and Thangavel, M. (2017). Isolation of fungi from the surface water of Vembanadu wetland agroecosystem. IJAMBR, 5: 52-58.

Watanabe, T. (2002). Pictorial atlas of soil and seed fungi morphologies of cultured fungi and key to species. 2nd Edition, CRC Press, 486pp.

Wichai, S.; Chuysinuan, P.; Chaiarwut, S.; Ekabutr, P. and Supaphol, P. (2019). Development of bacterial cellulose/alginate/chitosan composites incorporating copper(II) sulfate as an antibacterial wound dressing. J. Drug Deliv. Sci. Technol., 51: 662–671.

Wu, Z.; Huang, X.; Li, Y.C.; Xiao, H. and Wang, X. (2018). Novel chitosan films with laponite immobilized Ag nanoparticles for active food packaging. Carbohyd. Polym., 199: 210 –218.

Zhang, B.; Lv, D. and Fang, C. (2018). Chitooligosaccharide-metal ions complexes: Insights from molecular dynamics simulations. Colloid. Polym. Sci., 296: 245–250.